

Total Hadron-Hadron Cross Sections at High Energies

Wei-Ning Zhang^{1,2} and Cheuk-Yin Wong¹

¹*Physics Division, Oak Ridge National Laboratory, Oak Ridge, TN 37831, U.S.A.*

²*Department of Physics, Harbin Institute of Technology, Harbin, 150006, P. R. China*

(Dated: November 9, 2018)

We calculate total hadron-hadron cross sections at high energies using the Low-Nussinov two-gluon model of the Pomeron. The gluon exchange is represented by a phenomenological potential including screened color-Coulomb, screened confining, and spin-spin interactions. We use bound-state wave functions obtained from a potential model for mesons, and a Gaussian wave function for a proton. We evaluate total cross sections for collisions involving π , K , ρ , ϕ , D , J/ψ , ψ' , Υ , Υ' , and the proton. We find that the total cross sections increase with the square of the sum of the root-mean square radii of the colliding hadrons, but there are variations arising from the spin-spin interaction. We also calculate the total cross sections of a mixed-color charmonium state on a pion and on a proton. The dependence of the total cross section on the size and the color state of the charmonium is investigated.

PACS numbers: 13.85.Lg, 14.40.-n, 14.20.-c, 12.39.-x

I. INTRODUCTION

Hadron-hadron total cross sections are important characteristics of the dynamics of hadronic systems. Theoretical descriptions of the reaction process, however, remain incomplete as the mechanism of how hadrons interact contains important aspects of non-perturbative QCD. A phenomenological description of Donnachie and Landshoff [1] gives the total cross section in terms of the exchange of a Pomeron and a Reggeon. The exchange of a Pomeron dominates the cross section at high energies. It corresponds to the exchange of a tower of fictitious particles on a Regge trajectory with a Regge intercept of approximately 1. The exchange of a Reggeon dominates the cross section at low energies. It corresponds to the exchange of $\rho, \omega, f_2, a_2, \dots$ on the Regge trajectory with a Regge intercept of approximately 0.5.

It is desirable to study microscopic models of total hadron-hadron cross sections at high energies. The total cross sections provide useful information on the sizes of hadrons and the dynamics between them. Furthermore, they are important input data for the investigation of other reaction processes. For example, in high-energy heavy-ion collisions, the suppression of J/ψ production has been proposed as a signature for the production of the quark-gluon plasma [2]. However, the suppression of J/ψ production can also arise from the collision of J/ψ with hadrons at high energies. It is necessary to understand the absorption of J/ψ by hadrons before one can unambiguously identify the quark-gluon plasma as the source of J/ψ suppression [3, 4, 5, 6, 7, 8, 9, 10, 11, 12, 13, 14, 15, 16, 17, 18, 19, 20]. While the systematic studies of Donnachie and Landshoff provide very valuable information on the total cross section of many hadron-hadron systems, there are reactions (involving, for example, J/ψ) for which data are not available. They can only be evaluated theoretically [21, 22, 23, 24, 25, 26, 27]. It is therefore useful to develop a microscopic theory of hadron-hadron collisions at high energies.

As the Pomeron exchange is the dominant process in high-energy hadron-hadron reactions, it is useful to model the exchange of a Pomeron explicitly in microscopic terms. Previously, the Pomeron exchange in a hadron-hadron reaction was studied in terms of the exchange of two gluons. The two-gluon model of the Pomeron (TGMP), first proposed by Low [28] and Nussinov [29], was further investigated by Gunion and Soper [30] who introduced an effective gluon mass to mimic the confinement of the colored gluon. They examined the effects of the size of the bound-state hadrons and the number of quarks they contain. Landshoff and Nachtmann generalized the concept of the gluon condensate to the correlation length of the gluon field in the vacuum and discussed the short-range nature of the effective gluon exchange between quarks in hadron-hadron scattering [31]. The dependence of the cross sections on the sizes and the color states of the colliding hadrons was considered by Dolejši and Hüfner [32]. They obtained useful analytical and numerical results for the total cross sections of many hadron-hadron systems. The effects of channel coupling for the propagation of a radially-excited hadron [33] was investigated in the two-gluon model of the Pomeron by Wong [34] who also evaluated many meson-nucleon total cross sections.

We shall follow the approach of Gunion, Soper, Landshoff, Nachtmann, Dolejši, Hüfner, and Wong to study the hadron-hadron total cross section, with the following refinements. We shall use a set of meson wave functions obtained from meson mass calculations [18] to replace the simple form factors used in earlier studies. This allows a more detailed and systematic study of the hadron-hadron scattering processes involving a much large set of hadrons than those investigated previously. Gunion and Soper [30], Dolejši and Hüfner [32], and Wong [34] made use of only a single screened color-Coulomb potential to represent the non-perturbative gluon exchange. We shall instead represent the gluon exchange between the constituents of one hadron and constituents of the other hadron by a phenomenological

potential containing screened color-Coulomb, screened color-confining, and spin-spin interactions [18, 35, 36, 37]. Screening arises when the interaction between a constituent of one hadron and a constituent of another hadron occurs at large distances for which the production of dynamical quarks screens the interaction. The use of a more complicated potential allows a greater degree of flexibility, which provides a better description of non-perturbative effects in scattering. It also enables one to use reasonable strong interaction coupling constants, as the constraint of using a single screened color-Coulomb interaction may sometimes lead to values of α_s larger than unity [32]. In addition, the spin-spin interaction is known to be important in non-relativistic quark models. Its phenomenological incorporation here will allow us to evaluate the variation of the total cross section in reactions of mesons with different total spin quantum numbers and quarks of different flavors.

Similar to earlier works of Dolejši and Hüfner [32], and Wong [34], we shall first obtain the screening mass and the strength of the interaction to reproduce the experimental pp , πp , and Kp cross sections at $\sqrt{s} = 20$ GeV. We then use the theoretical meson wave functions to calculate other cross sections. Based on the energy dependence of the phenomenological description of total hadron-hadron cross sections found by Donnachie and Landshoff [1], we shall then extend our results to higher energies.

In reactions involving heavy quarkonium production in nuclear collisions, the initial heavy quark pair produced as a result of a parton-parton collision is a coherent state of a color admixture and different projections of this state will lead to different final heavy quarkonia [4, 38, 39, 40, 41, 42, 43]. We will also examine the color dependence of the cross section, in order to understand how a colored heavy quark pair propagates in a hadronic medium [4, 32, 39, 40, 41, 42, 43]. The nucleons with which the produced charmonium collide can also acquire a color as a result of prior collisions and may collide with a color-singlet charmonium [42, 43]. In this paper, we shall limit our discussion to the problem of the interaction of a colored charmonium state with a color-singlet hadron.

Our approach to study the total cross section in the TGMP differs from that of the additive quark model [44] and the dipole model of photoproduction [45]. The total cross sections obtained in different models can naturally be different. Careful comparison of these different results with experimental data will be useful to determine the importance of various scattering mechanisms that are present in the interaction of hadrons.

This paper is organized as follows. In Sec. II we describe the model used to calculate the hadron-hadron elastic scattering amplitude at high energies. In Sec. III we evaluate the spin matrix element for meson-meson, meson-proton, and proton-proton scattering. The calculation of the spatial matrix element is discussed in Sec. IV. In Sec. V we present results for total hadron-hadron cross sections and the energy dependence of the total hadron-hadron cross sections. In Sec. VI we evaluate the total cross sections of a mixed-color charmonium state scattering on a pion or a proton. The dependences of the total cross sections on the size and the color of the initial charmonium state are investigated. Finally, we present our summary and conclusions in Sec. VII.

II. TWO-GLUON MODEL OF THE POMERON

To calculate the total cross section in a hadron-hadron collision, we consider the hadron-hadron elastic scattering amplitude \mathcal{A} . According to the optical theorem, the imaginary part of the elastic scattering amplitude at zero momentum transfer gives the total hadron-hadron cross section.

The elastic scattering process between two hadrons at high energies is dominated by the exchange of a Pomeron, as evidenced by the slow variation of the total cross section with energy, the property of having an approximately purely imaginary forward scattering amplitude, and the dominance of no quantum number flow in the fragmentation region in forward inelastic processes. The phenomenological treatment of the total cross section as arising from the exchange of a Pomeron with a Regge trajectory intercept of 1.0808, and the exchange of a Reggeon from the trajectory of $\rho, \omega, f_2, a_2 \dots$ with an intercept of 0.5475, gives an excellent representation of many hadron-hadron total cross sections [1]. The small deviations of these Regge trajectory intercepts from the lowest-order expectations of 1.0 and 0.5 respectively have been attributed to higher-order effects [1].

In this work, we shall model the exchange of a Pomeron in terms of the exchange of gluons. As the exchange of a single gluon would lead to an exchange of color, the lowest number of gluon exchanges with no net color flow is the exchange of two gluons, proposed first by Low [28] and Nussinov [29] and studied by Gunion, Soper, Landshoff, Nachtmann, Dolejši, Hüfner, and Wong [30, 31, 32, 34].

Accordingly, we express the total hadron-hadron cross section in terms of the hadron-hadron elastic scattering amplitude at zero four-momentum transfer squared t

$$\sigma_{\text{tot}} = \frac{1}{s} \text{Im } \mathcal{A}(s, t = 0). \quad (1)$$

Following Gunion and Soper [30] and Dolejši and Hüfner [32], we obtain the forward scattering amplitude \mathcal{A} by including diagrams of the type shown in Fig. 1. As the elastic scattering process does not change the hadron internal

structure, the initial and final hadron states are identical. In Fig. 1, constituents i or j in hadron I interact with constituents k and l in hadron II by exchanging two gluons. As the elastic process involves important aspects of non-perturbative QCD, it is reasonable to represent the corresponding gluon exchange between constituents i and k in terms of a phenomenological potential $V(ik)$ possessing non-perturbative elements of color-Coulomb, confinement, and spin-spin interactions. The complete amplitude is obtained by summing over all possible diagrams representing the exchange of two gluons between all constituents $\{i, j\}$ of hadron I with all constituents $\{k, l\}$ of hadron II [32]:

$$\mathcal{A}(s, t) = \frac{is}{16} \sum_{i,j,k,l} \left\{ \int d^2\mathbf{b} e^{-i\mathbf{Q}\cdot\mathbf{b}} \left[\langle C_I C_{II} \chi_I \chi_{II} \Psi_I \Psi_{II} | V_T(ik) \right. \right. \\ \left. \left. \times V_T(jl) | C_I C_{II} \chi_I \chi_{II} \Psi_I \Psi_{II} \rangle \right] \right\}, \quad (2)$$

where \mathbf{b} is the impact parameter, $\mathbf{Q}^2 = -t$, C_I and C_{II} are the color wave functions, χ_I and χ_{II} are the spin wave functions, and Ψ_I and Ψ_{II} are the spatial wave functions of hadron I and hadron II, respectively. The square brackets represent the averaging over the color, spin, and internal spatial degrees of freedom of hadrons I and II. The sum $\sum_{i,j,k,l}$ is over all two-gluon exchange diagrams.

At high energies when the average intrinsic quark momentum inside a hadron is small compared to the center-of-mass energy, the case of a small momentum transfer in a two-gluon exchange diagram can be approximated as a loop diagram in which the quark lines on the loop can be treated as on the mass shell and represented by two delta functions (as in Eq. (A.11) of Ref. [31]). After integrating over the time-like and the longitudinal loop momenta using these two delta functions, the resultant effective gluon propagators involve only transverse momenta (or equivalently only transverse coordinates) [30, 31, 32]. When we represent the effective gluon propagator phenomenologically by an interaction, the interaction $V_T(ik)$ in transverse coordinates, written explicitly as $V_T(\mathbf{r}_T)$, can be obtained by integrating the interaction $V(\mathbf{r})$ over the longitudinal coordinate z ,

$$V_T(ik) = V_T(\mathbf{r}_T) = \int_{-\infty}^{\infty} dz V(\mathbf{r}), \quad (3)$$

where \mathbf{r} is the three-dimensional relative coordinate between the interacting particles i and k and \mathbf{r}_T its transverse component. Defining the Fourier transform of $V(\mathbf{r})$ as $\tilde{V}(\mathbf{k})$ by

$$V(\mathbf{r}) = \int \frac{d\mathbf{k}}{(2\pi)^3} e^{i\mathbf{k}\cdot\mathbf{r}} \tilde{V}(\mathbf{k}), \quad (4)$$

we can obtain from Eqs. (3) and (4)

$$V_T(\mathbf{r}_T) = \int \frac{d\mathbf{k}_T}{(2\pi)^2} e^{i\mathbf{k}_T\cdot\mathbf{r}_T} \tilde{V}(\mathbf{k}) \Big|_{k_z=0}. \quad (5)$$

Thus, $\tilde{V}_T(\mathbf{k}_T)$, the 2-dimensional Fourier transform of $V_T(\mathbf{r}_T)$, is just the 3-dimensional Fourier transform $\tilde{V}(\mathbf{k})$ evaluated at $k_z = 0$.

As the interaction between the constituents takes place at large distances, we are well advised to use a screened potential to represent the effects of dynamical quarks. As pointed out by Landshoff and Nachtmann [31], two quarks in two hadrons can exchange a nonperturbative gluon only if they pass within a short distance of each other. This short correlation length of the gluon field is another manifestation of the screening phenomenon. We employ screened color-Coulomb (Yukawa) and screened confining (exponential) potentials [35, 36, 37] and a spin-spin interaction [18, 35] for our interaction $V(\mathbf{r})$. The interaction between quark i in hadron I and quark k in hadron II in three-dimensional relative coordinate \mathbf{r} can be written as

$$V(\mathbf{r}) = \frac{\lambda_i}{2} \cdot \frac{\lambda_k}{2} \left\{ V_{\text{Yukawa}}(\mathbf{r}) + V_{\text{exponential}}(\mathbf{r}) + V_{\text{spin-spin}}(\mathbf{r}) \right\} \\ = \frac{\lambda_i}{2} \cdot \frac{\lambda_k}{2} \left\{ \frac{\alpha_s e^{-\mu r}}{r} + \frac{3b_0}{4\mu} e^{-\mu r} - \frac{8\pi\alpha_s}{3m_i m_k} (\mathbf{s}_i \cdot \mathbf{s}_k) \left(\frac{d^3}{\pi^{3/2}} \right) e^{-d^2 r^2} \right\}, \quad (6)$$

where λ_i is the Gell-Mann matrix, and λ_i is replaced by $-\lambda_i^T$ for an antiquark i . The quantities α_s , μ , b_0 , and d are the strong coupling constant, the effective screening parameter, the effective string-tension, and the spin-spin potential width parameter. The Fourier transform of the spatial and spin part of the potential is

$$\tilde{V}(\mathbf{k}) = \left[\frac{4\pi\alpha_s}{\mathbf{k}^2 + \mu^2} + \frac{6\pi b_0}{(\mathbf{k}^2 + \mu^2)^2} - \frac{8\pi\alpha_s}{3m_i m_k} \mathbf{s}_i \cdot \mathbf{s}_k e^{-\mathbf{k}^2/4d^2} \right]. \quad (7)$$

We have used an exponential interaction in Eq. (6) to represent the screened confining interaction as it contains the appropriate properties. At short distances for which screening effect is small, the exponential interaction gives the linear interaction $b_0 r$, and at large distances for which the confining interaction is screened by the production of dynamical quarks, it approaches zero. In terms of the Fourier transform, screening is represented by a non-vanishing value of the screening mass μ is Eq. (7). The use of a screened confining interaction is necessary here. If we assume an unscreened linear-confining interaction, corresponding to taking $\mu = 0$ in the $6\pi b_0/(\mathbf{k}_T + \mu^2)^2$ term in Eq. (7), we shall see in Section V that the total hadron-hadron cross section will be singular.

The square brackets in Eq. (2) can be written as

$$\begin{aligned} & \left[\langle C_I C_{II} \chi_I \chi_{II} \Psi_I \Psi_{II} | V_T(ik) V_T(jl) | C_I C_{II} \chi_I \chi_{II} \Psi_I \Psi_{II} \rangle \right] \\ &= \left\{ C_{ijkl} \sum_{a,b=1}^8 \langle C_I | \lambda_i^a \lambda_j^b | C_I \rangle \langle C_{II} | \lambda_k^a \lambda_l^b | C_{II} \rangle \right\} \left\{ \frac{1}{N_\chi} \sum_{\chi_{I,II}} \right. \\ & \left. \times \langle \chi_I \chi_{II} \Psi_I(\mathbf{r}_I) \Psi_{II}(\mathbf{r}_{II}) | V_T(\mathbf{r}_{IkT}) V_T(\mathbf{r}_{jIT}) | \chi_I \chi_{II} \Psi_I(\mathbf{r}_I) \Psi_{II}(\mathbf{r}_{II}) \rangle \right\}, \end{aligned} \quad (8)$$

where the first pair of curly brackets is the sum of color matrix elements, C_{ijkl} is the product of the four factors C_i , C_j , C_k , and C_l , each of which is 1 for a quark and -1 for an antiquark, and a and b are gluon color component labels. In the second pair of curly brackets, the sum is over all spin states of hadrons I and II (total number N_χ).

The color wave function for a color-singlet meson is

$$| C^1 \rangle = \frac{1}{\sqrt{3}} \sum_{\alpha=1}^3 | \alpha \bar{\alpha} \rangle, \quad (9)$$

where α ($\alpha = 1, 2, 3$) is the quark color label and $\bar{\alpha}$ is the corresponding antiquark color label. The color matrix element is

$$\langle C^1 | \lambda_m^a \lambda_n^b | C^1 \rangle = \frac{2}{3} \delta^{ab}. \quad (10)$$

For a color-singlet nucleon we have

$$| C^1 \rangle = \frac{1}{\sqrt{6}} \sum_{\alpha, \beta, \gamma=1}^3 \varepsilon_{\alpha\beta\gamma} | \alpha \beta \gamma \rangle, \quad (11)$$

and

$$\langle C^1 | \lambda_m^a \lambda_n^b | C^1 \rangle = \begin{cases} \frac{2}{3} \delta^{ab}, & \text{for } m = n, \\ -\frac{1}{3} \delta^{ab}, & \text{for } m \neq n. \end{cases} \quad (12)$$

III. SPIN MATRIX ELEMENTS

From Eqs. (2) and (6), the matrix element for the spatial and spin part can be separated into a sum of products of spin matrix elements and spatial matrix elements. The first-order spin-spin matrix elements and the second-order spin-spin matrix elements are

$$s_{ik}^{(1)} = \langle \chi_I \chi_{II} | (\mathbf{s}_i \cdot \mathbf{s}_k) | \chi_I \chi_{II} \rangle, \quad (13)$$

$$s_{ikjl}^{(2)} = \langle \chi_I \chi_{II} | (\mathbf{s}_i \cdot \mathbf{s}_k)(\mathbf{s}_j \cdot \mathbf{s}_l) | \chi_I \chi_{II} \rangle. \quad (14)$$

We shall give results for these quantities for meson-meson, meson-proton, and proton-proton collisions separately.

A. The meson–meson case

Consider meson I with constituents i and j coupled to total spin S_I , and meson II with constituents k and l coupled to total spin S_{II} . We would like to recouple the constituents so that the operators $(\mathbf{s}_i \cdot \mathbf{s}_k)$ and $(\mathbf{s}_j \cdot \mathbf{s}_l)$ have simple eigenvalues. We have

$$\begin{aligned}
|\chi_I \chi_{II}\rangle &= |(ij)_{S_{Iz}}^{S_I} (kl)_{S_{IIz}}^{S_{II}}\rangle = \sum_{S, S_z} (SS_z | S_I S_{Iz} S_{II} S_{IIz}) | [(ij)^{S_I} (kl)^{S_{II}}]_{S_z}^S \rangle \\
&= \sum_{S, S_z} \sum_{S_{ik}, S_{jl}} (SS_z | S_I S_{Iz} S_{II} S_{IIz}) \hat{S}_I \hat{S}_{II} \hat{S}_{ik} \hat{S}_{jl} \begin{Bmatrix} s_i & s_j & S_I \\ s_k & s_l & S_{II} \\ S_{ik} & S_{jl} & S \end{Bmatrix} | [(ik)^{S_{ik}} (jl)^{S_{jl}}]_{S_z}^S \rangle \\
&= \sum_{S, S_z} \sum_{S_{il}, S_{jk}} (SS_z | S_I S_{Iz} S_{II} S_{IIz}) (-1)^{S_{II}-s_k-s_l} \hat{S}_I \hat{S}_{II} \hat{S}_{il} \hat{S}_{jk} \begin{Bmatrix} s_i & s_j & S_I \\ s_l & s_k & S_{II} \\ S_{il} & S_{jk} & S \end{Bmatrix} \\
&\quad \times | [(il)^{S_{il}} (jk)^{S_{jk}}]_{S_z}^S \rangle,
\end{aligned} \tag{15}$$

where $\hat{S} = \sqrt{2S+1}$. From the above equation, the matrix element $s_{ik}^{(1)} = \langle \chi_I \chi_{II} | (\mathbf{s}_i \cdot \mathbf{s}_k) | \chi_I \chi_{II} \rangle$ is

$$s_{ik}^{(1)} = \sum_{S, S_z} \sum_{S_{ik}, S_{jl}} |(SS_z | S_I S_{Iz} S_{II} S_{IIz})|^2 \hat{S}_I^2 \hat{S}_{II}^2 \hat{S}_{ik}^2 \hat{S}_{jl}^2 \begin{Bmatrix} s_i & s_j & S_I \\ s_k & s_l & S_{II} \\ S_{ik} & S_{jl} & S \end{Bmatrix}^2 \frac{1}{2} [S_{ik}(S_{ik}+1) - \frac{3}{2}], \tag{16}$$

and the matrix element $s_{ikjl}^{(2)} = \langle \chi_I \chi_{II} | (\mathbf{s}_i \cdot \mathbf{s}_k)(\mathbf{s}_j \cdot \mathbf{s}_l) | \chi_I \chi_{II} \rangle$ are

$$s_{ikik}^{(2)} = \sum_{S, S_z} \sum_{S_{ik}, S_{jl}} |(SS_z | S_I S_{Iz} S_{II} S_{IIz})|^2 \hat{S}_I^2 \hat{S}_{II}^2 \hat{S}_{ik}^2 \hat{S}_{jl}^2 \begin{Bmatrix} s_i & s_j & S_I \\ s_k & s_l & S_{II} \\ S_{ik} & S_{jl} & S \end{Bmatrix}^2 \left\{ \frac{1}{2} [S_{ik}(S_{ik}+1) - \frac{3}{2}] \right\}^2, \tag{17}$$

$$\begin{aligned}
s_{ikil}^{(2)} &= \sum_{S, S_z} \sum_{S_{ik}, S_{jl}} \sum_{S_{il}, S_{jk}} |(SS_z | S_I S_{Iz} S_{II} S_{IIz})|^2 (-1)^{S_{II}-s_k-s_l} (-1)^{S_{jl}-s_j-s_l} (-1)^{S_{jk}-s_j-s_k} \\
&\quad \times \hat{S}_I^2 \hat{S}_{II}^2 \hat{S}_{ik}^2 \hat{S}_{jl}^2 \hat{S}_{il}^2 \hat{S}_{jk}^2 \begin{Bmatrix} s_i & s_j & S_I \\ s_k & s_l & S_{II} \\ S_{ik} & S_{jl} & S \end{Bmatrix} \begin{Bmatrix} s_i & s_k & S_{ik} \\ s_l & s_j & S_{jl} \\ S_{il} & S_{jk} & S \end{Bmatrix} \begin{Bmatrix} s_i & s_j & S_I \\ s_l & s_k & S_{II} \\ S_{il} & S_{jk} & S \end{Bmatrix} \\
&\quad \times \frac{1}{2} [S_{ik}(S_{ik}+1) - \frac{3}{2}] \times \frac{1}{2} [S_{il}(S_{il}+1) - \frac{3}{2}], \quad \text{for } k \neq l,
\end{aligned} \tag{18}$$

$$\begin{aligned}
s_{ikjl}^{(2)} &= \sum_{S, S_z} \sum_{S_{ik}, S_{jl}} |(SS_z | S_I S_{Iz} S_{II} S_{IIz})|^2 \hat{S}_I^2 \hat{S}_{II}^2 \hat{S}_{ik}^2 \hat{S}_{jl}^2 \begin{Bmatrix} s_i & s_j & S_I \\ s_k & s_l & S_{II} \\ S_{ik} & S_{jl} & S \end{Bmatrix}^2 \frac{1}{2} [S_{ik}(S_{ik}+1) - \frac{3}{2}] \\
&\quad \times \frac{1}{2} [S_{jl}(S_{jl}+1) - \frac{3}{2}], \quad \text{for } i \neq j \text{ and } k \neq l,
\end{aligned} \tag{19}$$

where $i, j = 1, 2$; $k, l = 3, 4$.

B. The meson–proton and proton–proton cases

The spin and flavor wave function for a proton in the $S_z = 1/2$ state is

$$\begin{aligned}
|p_{1/2}^{1/2}\rangle &= \frac{1}{\sqrt{18}} \left(2|u_+u_+d_-\rangle - |u_+u_-d_+\rangle - |u_-u_+d_+\rangle \right. \\
&\quad + 2|u_+d_-u_+\rangle - |u_+d_+u_-\rangle - |u_-d_+u_+\rangle \\
&\quad \left. + 2|d_-u_+u_+\rangle - |d_+u_+u_-\rangle - |d_+d_-u_+\rangle \right).
\end{aligned} \tag{20}$$

Denoting the two u -quarks by 3 and 4, the d -quark by 5, and the spinor of quark i as $i_{s_z}^s$, we have

$$\begin{aligned} |p_{1/2}^{1/2}\rangle = \frac{1}{\sqrt{18}} & \left(2 |3_{1/2}^{1/2} 4_{1/2}^{1/2} 5_{-1/2}^{1/2}\rangle - |3_{1/2}^{1/2} 4_{-1/2}^{1/2} 5_{1/2}^{1/2}\rangle - |3_{-1/2}^{1/2} 4_{1/2}^{1/2} 5_{1/2}^{1/2}\rangle \right. \\ & + 2 |3_{1/2}^{1/2} 5_{-1/2}^{1/2} 4_{1/2}^{1/2}\rangle - |3_{1/2}^{1/2} 5_{1/2}^{1/2} 4_{-1/2}^{1/2}\rangle - |3_{-1/2}^{1/2} 5_{1/2}^{1/2} 4_{1/2}^{1/2}\rangle \\ & \left. + 2 |5_{-1/2}^{1/2} 3_{1/2}^{1/2} 4_{1/2}^{1/2}\rangle - |5_{1/2}^{1/2} 3_{1/2}^{1/2} 4_{-1/2}^{1/2}\rangle - |5_{1/2}^{1/2} 3_{-1/2}^{1/2} 4_{1/2}^{1/2}\rangle \right). \end{aligned} \quad (21)$$

We can couple the spin of any two of 3, 4, and 5. For example, coupling 3 and 4, we have

$$\begin{aligned} |p_{1/2}^{1/2}\rangle = \frac{1}{\sqrt{18}} & \left[2 \left(\frac{1}{2} \frac{1}{2} \frac{1}{2} \frac{1}{2} \right) \left(|3_{1/2}^1 5_{-1/2}^{1/2}\rangle_{(1)} + |3_{4/2}^1 5_{-1/2}^{1/2}\rangle_{(4)} + |3_{(4)}^1 5_{-1/2}^{1/2}\rangle_{(7)} \right) \right. \\ & - \sum_{S_{34}, S_{34z}} \left(\frac{1}{2} \frac{1}{2} \frac{1}{2} - \frac{1}{2} \right) \left| S_{34} S_{34z} \right\rangle \left(|3_{S_{34z}}^{S_{34}} 5_{1/2}^{1/2}\rangle_{(2)} - |3_{S_{34z}}^{S_{34}} 5_{1/2}^{1/2}\rangle_{(5)} \right. \\ & \quad \left. - |3_{S_{34z}}^{S_{34}} 5_{1/2}^{1/2}\rangle_{(8)} \right) \\ & + \sum_{S_{34}, S_{34z}} \left(\frac{1}{2} - \frac{1}{2} \frac{1}{2} \frac{1}{2} \right) \left| S_{34} S_{34z} \right\rangle \left(|3_{S_{34z}}^{S_{34}} 5_{1/2}^{1/2}\rangle_{(3)} - |3_{S_{34z}}^{S_{34}} 5_{1/2}^{1/2}\rangle_{(6)} \right. \\ & \quad \left. - |3_{S_{34z}}^{S_{34}} 5_{1/2}^{1/2}\rangle_{(9)} \right) \left. \right] \\ \equiv & |3_{(4)} 5\rangle, \end{aligned} \quad (22)$$

where the subscript (n) labels the flavor component in the n -th term in Eq. (21) (i.e., ${}_{(n)}\langle (kl)_{S_{klz}}^{S_{kl}} l' | (kl)_{S_{klz}}^{S_{kl}} l' \rangle_{(n')} = \delta(S_{klz} S_{klz}') \delta(S_{kl} S_{kl}') \delta(nn')$). We can also write out the other coupling expressions of $|p_{1/2}^{1/2}\rangle$, for example, $|3_{(5)} 4\rangle$ and $|4_{(5)} 3\rangle$. One can obtain a similar decomposition for $|p_{-1/2}^{1/2}\rangle$.

Thus, the first-order and second-order spin-spin matrix elements for a meson-proton scattering can be expressed as

$$\begin{aligned} s_{ik}^{(1)} &= \langle (ij)_{S_z}^{S_i} [(kl) l'] | (s_i \cdot s_k) | (ij)_{S_z}^{S_i} [(kl) l'] \rangle \\ &= \langle (ij)_{S_z}^{S_i} (kl) | (s_i \cdot s_k) | (ij)_{S_z}^{S_i} (kl) \rangle, \end{aligned} \quad (23)$$

$$\begin{aligned} s_{ikjl}^{(2)} &= \langle (ij)_{S_z}^{S_i} [(kl) l'] | (s_i \cdot s_k)(s_j \cdot s_l) | (ij)_{S_z}^{S_i} [(kl) l'] \rangle \\ &= \langle (ij)_{S_z}^{S_i} (kl) | (s_i \cdot s_k)(s_j \cdot s_l) | (ij)_{S_z}^{S_i} (kl) \rangle, \end{aligned} \quad (24)$$

where l' is a spectator, $i, j = 1, 2$, and $k, l = 3, 4, 5$. Each term in Eqs. (23) and (24) can be calculated in the same way as in the meson-meson case. For a proton-proton scattering, we have

$$\begin{aligned} s_{ik}^{(1)} &= \langle [(ij) j'] [(kl) l'] | (s_i \cdot s_k) | [(ij) j'] [(kl) l'] \rangle \\ &= \langle (ij) (kl) | (s_i \cdot s_k) | (ij) (kl) \rangle, \end{aligned} \quad (25)$$

$$\begin{aligned} s_{ikjl}^{(2)} &= \langle [(ij) j'] [(kl) l'] | (s_i \cdot s_k)(s_j \cdot s_l) | [(ij) j'] [(kl) l'] \rangle \\ &= \langle (ij) (kl) | (s_i \cdot s_k)(s_j \cdot s_l) | (ij) (kl) \rangle, \end{aligned} \quad (26)$$

where j' and l' are spectators, $i, j = 1, 2, 3$, and $k, l = 4, 5, 6$. Each term in Eqs. (25) and (26) can be calculated similar to the meson-meson case.

IV. SPATIAL MATRIX ELEMENTS

A. The meson-meson case

Using a set of Gaussian basis states with different widths, Wong *et al.* previously obtained bound-state meson wave functions from a non-relativistic quark model [18]. The model assumes color-Coulomb, linear-confining, and spin-spin

interactions. It gives meson masses in reasonable agreement with experimental data. The meson wave functions are tabulated in Table IV of Ref. [18]. We shall use these meson wave functions in our calculations. They are represented by a nonorthogonal sum of Gaussian basis functions of different widths,

$$\Psi(\mathbf{r}) = \sum_{n=1}^6 a_n \phi_n(\mathbf{r}) = \sum_{n=1}^6 a_n \left(\frac{n\beta^2}{\pi}\right)^{3/4} e^{-\frac{n\beta^2}{2}r^2}, \quad (27)$$

where $\mathbf{r} = (\mathbf{r}_T, z)$ is the three-dimensional coordinate, a_n is the coefficient of the n -th component, and β is a parameter characterizing the width of the basis functions in momentum space.

The transverse coordinates of the quarks and antiquarks in meson I and II can be expressed as

$$\mathbf{r}_{1T,2T} = \frac{\mathbf{b}}{2} \pm \frac{\mathbf{r}_{IT}}{2}, \quad \mathbf{r}_{3T,4T} = -\frac{\mathbf{b}}{2} \pm \frac{\mathbf{r}_{IIT}}{2}, \quad (28)$$

where \mathbf{r}_{IT} or \mathbf{r}_{IIT} is the relative transverse coordinate of the quark and antiquark in meson I or II respectively. The relative transverse coordinate of quark (or antiquark) i in meson I and quark (or antiquark) k in meson II can be expressed as

$$\begin{aligned} \mathbf{r}_{ikT} &= \mathbf{r}_{iT} - \mathbf{r}_{kT} = \mathbf{b} + \frac{C_{Ii}}{2}\mathbf{r}_{IT} + \frac{C_{IIk}}{2}\mathbf{r}_{IIT}, \\ (i &= 1, 2, \quad k = 3, 4, \quad C_{I1} = 1, \quad C_{I2} = -1, \quad C_{II3} = -1, \quad C_{II4} = 1.) \end{aligned} \quad (29)$$

From Eqs. (2), (5), (8), (27), and (29), the spatial matrix element for a meson-meson scattering is

$$\begin{aligned} &\int d^2\mathbf{b} e^{-i\mathbf{Q}\cdot\mathbf{b}} \int d\mathbf{r}_I d\mathbf{r}_{II} \Psi_{I,f}^*(\mathbf{r}_I) \Psi_{II,f}^*(\mathbf{r}_{II}) V_T(\mathbf{r}_{ikT}) V_T(\mathbf{r}_{jlT}) \Psi_{I,i}(\mathbf{r}_I) \Psi_{II,i}(\mathbf{r}_{II}) \\ &= \frac{1}{(2\pi)^2} \int d^2\mathbf{k}_T \tilde{V}_T(\mathbf{k}_T) \tilde{V}_T(\mathbf{k}_T - \mathbf{Q}) F_{ij}^M(\mathbf{Q}, \mathbf{k}_T) F_{kl}^M(\mathbf{Q}, \mathbf{k}_T), \quad (i, j = 1, 2; k, l = 3, 4), \end{aligned} \quad (30)$$

where the superscript in $F_{kl}^M(\mathbf{Q})$ labels the colliding hadron as a meson M or proton P, and

$$F_{ij}^M(\mathbf{Q}, \mathbf{k}_T) = \sum_{n,n'} a_n a_{n'} \left(\frac{2\sqrt{nn'}}{n+n'}\right)^{3/2} \exp\left\{-\frac{[\mathbf{k}_T + C_{Ii}C_{Ij}(\mathbf{Q} - \mathbf{k}_T)]^2}{8(n+n')\beta_I^2}\right\}, \quad (31)$$

$$F_{kl}^M(\mathbf{Q}, \mathbf{k}_T) = \sum_{m,m'} a_m a_{m'} \left(\frac{2\sqrt{mm'}}{m+m'}\right)^{3/2} \exp\left\{-\frac{[\mathbf{k}_T + C_{IIk}C_{IIl}(\mathbf{Q} - \mathbf{k}_T)]^2}{8(m+m')\beta_{II}^2}\right\}. \quad (32)$$

B. The meson–proton and proton–proton case

The three-dimensional coordinate \mathbf{r}_k of a quark in a proton can be written in terms of Jacobi coordinates $\boldsymbol{\eta} = (\boldsymbol{\eta}_T, \eta_z)$ and $\boldsymbol{\xi} = (\boldsymbol{\xi}_T, \xi_z)$ [32]. Its transverse component is given by

$$\mathbf{r}_{kT} = -\frac{\mathbf{b}}{2} + \frac{\delta_{IIk}}{6}\boldsymbol{\eta}_T + \frac{C_{IIk}}{2}\boldsymbol{\xi}_T, \quad (33)$$

where

$$\delta_{IIk} = \begin{cases} 2, & k = 3, \\ -1, & k = 4, 5, \end{cases} \quad C_{IIk} = \begin{cases} 0, & k = 3, \\ 1, & k = 4, \\ -1, & k = 5. \end{cases} \quad (34)$$

The relative transverse coordinate of the quark (or antiquark) i in meson I and the quark k in proton II is

$$\mathbf{r}_{ikT} = \mathbf{r}_{iT} - \mathbf{r}_{kT} = \mathbf{b} + \frac{C_{Ii}}{2}\mathbf{r}_{IT} - \frac{\delta_{IIk}}{6}\boldsymbol{\eta}_T - \frac{C_{IIk}}{2}\boldsymbol{\xi}_T. \quad (35)$$

We use a simple Gaussian wave function for a proton. In terms of Jacobi coordinates, it can be expressed as [32]

$$\Psi(\boldsymbol{\eta}, \boldsymbol{\xi}) = (24\sqrt{3}\pi^3 \langle r_p^2 \rangle^3)^{-1/2} \exp[(-\boldsymbol{\eta}^2/12 - \boldsymbol{\xi}^2/4)/\langle r_p^2 \rangle]. \quad (36)$$

From Eqs. (2), (5), (8), (27), and (34) — (36), the spatial matrix element for a meson-proton scattering is

$$\begin{aligned} & \int d^2\mathbf{b} e^{-i\mathbf{Q}\cdot\mathbf{b}} \int d\mathbf{r}_I d\boldsymbol{\eta} d\boldsymbol{\xi} \Psi_{I,f}^*(\mathbf{r}_I) \Psi_{II,f}^*(\boldsymbol{\eta}, \boldsymbol{\xi}) V_T(\mathbf{r}_{IkT}) V_T(\mathbf{r}_{jIT}) \Psi_{I,i}(\mathbf{r}_I) \Psi_{II,i}(\boldsymbol{\eta}, \boldsymbol{\xi}) \\ &= \frac{1}{(2\pi)^2} \int d^2\mathbf{k}_T \tilde{V}_T(\mathbf{k}_T) \tilde{V}_T(\mathbf{k}_T - \mathbf{Q}) F_{ij}^M(\mathbf{Q}, \mathbf{k}_T) F_{kl}^P(\mathbf{Q}, \mathbf{k}_T), \\ & \quad (i, j = 1, 2; k, l = 3, 4, 5), \end{aligned} \quad (37)$$

where

$$F_{kl}^P(\mathbf{Q}, \mathbf{k}_T) = \begin{cases} \exp\left(-\frac{\langle r_p^2 \rangle}{6} \mathbf{Q}^2\right), & k = l, \\ \exp\left\{-\frac{\langle r_p^2 \rangle}{6} [\mathbf{Q}^2 - \frac{3}{2} \mathbf{Q} \cdot (2\mathbf{k}_T) + \frac{3}{4} (2\mathbf{k}_T)^2]\right\}, & k \neq l. \end{cases} \quad (38)$$

For a proton-proton scattering, the spatial matrix element is

$$\begin{aligned} & \int d^2\mathbf{b} e^{-i\mathbf{Q}\cdot\mathbf{b}} \int d\boldsymbol{\eta}_I d\boldsymbol{\xi}_I d\boldsymbol{\eta}_{II} d\boldsymbol{\xi}_{II} \Psi_{I,f}^*(\boldsymbol{\eta}_I, \boldsymbol{\xi}_I) \Psi_{II,f}^*(\boldsymbol{\eta}_{II}, \boldsymbol{\xi}_{II}) V_T(\mathbf{r}_{IkT}) V_T(\mathbf{r}_{jIT}) \Psi_{I,i}(\boldsymbol{\eta}_I, \boldsymbol{\xi}_I) \Psi_{II,i}(\boldsymbol{\eta}_{II}, \boldsymbol{\xi}_{II}) \\ &= \frac{1}{(2\pi)^2} \int d^2\mathbf{k}_T \tilde{V}_T(\mathbf{k}_T) \tilde{V}_T(\mathbf{k}_T - \mathbf{Q}_T) F_{ij}^P(\mathbf{Q}, \mathbf{k}_T) F_{kl}^P(\mathbf{Q}, \mathbf{k}_T), \quad (i, j = 1, 2, 3; k, l = 4, 5, 6). \end{aligned} \quad (39)$$

V. TOTAL HADRON-HADRON CROSS SECTIONS

After we have evaluated the color matrix element, the spin matrix element, and the spatial matrix element, we can now determine the total hadron-hadron cross section as

$$\sigma_{\text{tot}} = \frac{1}{16} \sum_{i,j,k,l} C_{f,ijkl} I_{ijkl}, \quad (40)$$

where

$$C_{f,ijkl} = C_{ijkl} \sum_{a,b=1}^8 \langle C_I | \lambda_i^a \lambda_j^b | C_I \rangle \langle C_{II} | \lambda_k^a \lambda_l^b | C_{II} \rangle, \quad (41)$$

$$\begin{aligned} I_{ijkl} &= \frac{1}{(2\pi)^2} \int d^2\mathbf{k}_T \tilde{V}_T(\mathbf{k}_T) \tilde{V}_T(\mathbf{k}_T) F_{ij}^I(\mathbf{Q} = 0, \mathbf{k}_T) F_{kl}^{II}(\mathbf{Q} = 0, \mathbf{k}_T) \\ &= \frac{1}{(2\pi)^2} \int d^2\mathbf{k}_T \left\{ \left[\frac{4\pi\alpha_s}{\mathbf{k}_T^2 + \mu^2} + \frac{6\pi b_0}{(\mathbf{k}_T^2 + \mu^2)^2} \right]^2 \right. \\ & \quad \left. + \langle s_{ikjl}^{(2)} \rangle \frac{(8\pi\alpha_s)^2}{9m_i m_k m_j m_l} e^{-\mathbf{k}_T^2/2d^2} \right\} F_{ij}^I(\mathbf{Q} = 0, \mathbf{k}_T) F_{kl}^{II}(\mathbf{Q} = 0, \mathbf{k}_T). \end{aligned} \quad (42)$$

The superscript I (or II) is either M (meson) or P (proton), and $\langle s_{ikjl}^{(2)} \rangle$ is the second-order spin-spin matrix element averaged over all polarization states of hadrons I and II,

$$\langle s_{ikjl}^{(2)} \rangle = \frac{1}{N_\chi} \sum_{\chi_{I,II}} \langle \chi_I \chi_{II} | (\mathbf{s}_i \cdot \mathbf{s}_k)(\mathbf{s}_j \cdot \mathbf{s}_l) | \chi_I \chi_{II} \rangle. \quad (43)$$

The polarization average of the first-order spin-spin matrix elements $\langle s_{ik}^{(1)} \rangle$ is zero.

If we assume an unscreened linear-confining interaction for hadron-hadron collision (which corresponds to taking $\mu = 0$ in the $6\pi b_0/(\mathbf{k}_T + \mu^2)^2$ term in Eq. (42)), the total cross section will be singular, since the integral over \mathbf{k}_T in Eq.

(42) diverges. From a physical viewpoint, we expect the interaction between constituents in different hadrons to occur at relatively large separations. As a consequence, the interaction will be subject to screening, due to the production of virtual $q\bar{q}$ pairs. The linear confining interaction for bound states should thus become a screened confining potential when applied to the interactions of quarks in a diffractive hadron-hadron scattering process. Similarly we expect the color-Coulomb interaction to be screened. The spatial dependence of the interaction in Eq. (6) between quarks and antiquarks of different hadrons should be different from those inside the same hadron.

A simple way to incorporate screening is to replace \mathbf{k}^2 in the Fourier transforms of the color-Coulomb and the linear interactions by $\mathbf{k}^2 + \mu^2$, which leads respectively to the Yukawa and exponential potentials, as given in Eqs. (6) and (7) and the interaction in Eq. (42). Previously, in studying the screened potential and its temperature dependence inferred from lattice gauge theory, the effective string tension $b_0 = 0.35 \text{ GeV}^2$ was found to give good descriptions of meson bound state masses [35]. We shall use this effective string tension in the present work.

The rms radii of hadrons are model-dependent as the interactions are sometimes implicitly included in the determination of the effective rms radius. We shall use the meson bound state wave functions obtained in the non-relativistic quark model of Ref. [18], where the rms radius is 0.256 fm for a pion and 0.261 fm for a kaon. (See Table IV of Ref. [18], in which the quantity $\sqrt{\langle r^2 \rangle}$ in the fourth column is the rms $q-\bar{q}$ separation, which is twice the rms meson radius.) In our present model in which a hadron-hadron reaction takes place via a finite-range interaction between constituents in one hadron with constituents of the other hadron, these hadron constituent radii can be considered “core” radii. These pion and kaon rms “core” radii are smaller than the corresponding values of 0.61 fm and 0.54 fm found in the geometrical model of Chou and Yang [46, 47] as well as the values of 0.56 fm and 0.53 fm determined from electromagnetic measurements [48, 49]. These differences arise from the fact that Chou and Yang describe hadrons as a geometrical droplet with an essentially local zero-range interaction between a constituent of one hadron with the constituent of the other hadron. In the electromagnetic measurement, the photon also fluctuates into a ρ meson, and the larger electromagnetic rms radii include the additional effects of this fluctuation.

It is reasonable to assume that the hadron radius $r_{\text{hadron}}(\text{EM})$, obtained in an electromagnetic measurement, is the sum of the hadron radius used here (the core radius) and an effective rho meson radius (which is of order $1/m_\rho$),

$$r_{\text{hadron}}(\text{EM}) = (\text{hadron core radius}) + (\text{effective } \rho \text{ meson radius}). \quad (44)$$

Based on this assumption, the difference of of the proton and pion rms electromagnetic radii is equal to the difference of their corresponding rms (core) radii,

$$\sqrt{\langle r_p^2(\text{EM}) \rangle} - \sqrt{\langle r_\pi^2(\text{EM}) \rangle} = \sqrt{\langle r_p^2 \rangle} - \sqrt{\langle r_\pi^2 \rangle}. \quad (45)$$

The proton and pion rms radius obtained in electromagnetic measurements are 0.81 fm [50] and 0.56 fm [48] respectively. Using the meson bound states wave functions in Ref. [18] for which $\sqrt{\langle r_\pi^2 \rangle} = 0.256 \text{ fm}$, the above relation gives a proton rms radius of $\sqrt{\langle r_p^2 \rangle} = 0.51 \text{ fm}$ which we shall adopt in our present analysis. This value of the proton rms radius is close to the value of $\sqrt{\langle r_p^2 \rangle} = 0.48 \text{ fm}$ found by Copley, Karl, and Obryk [51], and Koniuk and Isgur [52] in their quark-model description of baryon electromagnetic transition amplitudes. We shall use the quark masses and the hyperfine smearing parameter d that are employed in the meson bound state wave function calculations in Ref.[18]: $m_u = m_d = 0.334 \text{ GeV}$, $m_s = 0.575 \text{ GeV}$, $m_c = 1.776 \text{ GeV}$, $m_b = 5.102 \text{ GeV}$, and $d = 0.897 \text{ GeV}$.

We search for the screening mass μ and the strong coupling constant parameter α_s by fitting the experimental cross sections of $\sigma_{\text{tot}}(p+p) = 39.0 \text{ mb}$, $\sigma_{\text{tot}}(\pi+p) = 24.0 \text{ mb}$, and $\sigma_{\text{tot}}(K+p) = 20.5 \text{ mb}$ at $\sqrt{s} = 20 \text{ GeV}$ [53]. We obtain $\mu = 0.425 \text{ GeV}$, and $\alpha_s = 0.495$ by using the Levenberg-Marquardt method [54].

The screening mass $\mu = 0.425 \text{ GeV}$ falls in between m_π and m_ρ studied by Dolejši and Hüfner [32]. It is interesting to note from Fig. 3 of their work that a screening mass between m_π and m_ρ gives the best correlation between the total cross section and the effective elastic scattering slope parameter b_{eff} . It is therefore important to extend the present calculations to the analysis of elastic scattering in future work.

The screening length $1/\mu = 0.464 \text{ fm}$ is the same physical quantity as the correlation length a studied by Landshoff and Nachtmann [31]. Using a single gluon propagator with a screening mass μ , they noted that $1/\mu$ must be much smaller than the radius of a hadron, for the additive quark model to be valid. Our numerical analysis, with the full non-perturbative interaction of Eq. (6), leads to a range $1/\mu$ that is not small compared to the radius of a hadron; we should not expect our results to coincide completely with those of the additive quark model in all aspects.

The value of $\alpha_s = 0.495$ is slightly smaller but close to the conventional strong interaction coupling constant of $\alpha_s = 0.6$ used in non-relativistic quark models for light quarks [21].

We shall first focus our attention on the total hadron-hadron cross sections at $\sqrt{s} = 20 \text{ GeV}$ in Fig. 2 and then discuss the energy dependence in Eqs. (54)-(56) and Fig. 3. The experimental pp , πp , and Kp total cross sections at $\sqrt{s} = 20 \text{ GeV}$ can be roughly represented by $\sigma_{\text{tot}} \sim 5.86(\sqrt{\langle r_I^2 \rangle} + \sqrt{\langle r_{II}^2 \rangle})^2$. While the theoretical total cross

sections obtained in the present TGMP calculations tend to increase with the square of the sum of the rms radii, there are however variations that arise from the spin-spin interaction. The latter quantity depends on the masses of the interacting quarks and the strength of the spin-spin interaction involving strange quarks is smaller than that of light quarks; consequently, $\sigma_{\text{tot}}(\pi + p) > \sigma_{\text{tot}}(K + p)$, as shown in Fig. 2.

Our total cross section for $\rho + p$ at $\sqrt{s} = 20$ GeV is 27.0 mb, which is slightly larger than the total $\pi + p$ cross section of 24.5 mb. In the TGMP, the spin-spin interaction affects the ρ meson cross sections in two ways. First, as the quark-antiquark potential is weaker for the ρ meson than for the pion due to the spin-spin interaction, the ρ rms radius is 0.385 fm, which is substantially larger than the pion rms radius of 0.256 fm. Secondly, the spin-spin interaction also affects the interaction strength between a quark or antiquark in the ρ meson and a constituent in the other hadron. Hence, the TGMP predicts $\sigma_{\text{tot}}(\rho + p)$ slightly greater than $\sigma_{\text{tot}}(\pi + p)$. This result is slightly greater than the prediction of the additive quark model which gives

$$\sigma_{\text{tot}}(\rho + p)(\text{additive quark model}) = \frac{1}{2}[\sigma_{\text{tot}}(\pi^+ + p) + \sigma_{\text{tot}}(\pi^- + p)] \sim 24.2 \text{ mb.} \quad (46)$$

It is interesting to note that our TGMP total cross sections for $\pi + \pi$, and $\rho + \pi$ are respectively 27.4 and 20.8 mb, which are significantly larger than the predictions of about $2\sigma_{\text{tot}}(\pi + N)/3 \sim 16$ mb from the additive quark model. The large magnitude of the total cross sections in the present calculation arises from the spin-spin interaction, as the cross sections become much smaller if the spin-spin interaction is turned off.

Experimental information of the $\rho + p$ cross section can be inferred from ρ -meson photoproduction cross sections. The extracted total cross section depends on the coupling constant $f_\rho^2/4\pi$ and the value of η_ρ , which is the ratio of the real and imaginary parts of the scattering amplitude [55]. It also depends on the generalizations of the Vector Dominance Model in which one may include higher resonances and off-diagonal matrix elements [56, 57].

Using the simple VDM with η_ρ assumed to be zero and $f_\rho^2/4\pi$ set to be 2.20, the ZEUS Collaboration found

$$\sigma_{\text{tot}}(\rho_0 + p) = 28.0 \pm 1.2 \text{ mb} \quad (47)$$

for $\sqrt{s} = 70$ GeV [58] which is close to the value of $\sigma_{\text{tot}}(\rho + p) = 30.5$ mb obtained in the present calculation for $\sqrt{s} = 70$ GeV (see Fig. 3).

At low energies, the experimental data cannot be compared directly with the present theoretical prediction. One can nevertheless get some idea on the magnitude of $\sigma_{\text{tot}}(\rho + p)$. Using photoproduction data from a number of different nuclei, McClellan *et al.* [59] found earlier

$$\sigma_{\text{tot}}(\rho_0 + p) = 38.0 \pm 3 \text{ mb} \quad (48)$$

and $f_\rho^2/4\pi = 4.40 \pm 0.60$ for photons at 6 GeV ($\sqrt{s} = 3.48$ GeV). However, from their subsequent extended measurements and refined analysis they obtain

$$\sigma_{\text{tot}}(\rho_0 + p) = 25.9 \pm 1 \text{ mb} \quad (49)$$

and $f_\rho^2/4\pi = 2.52 \pm 0.08$ with $\eta = -0.24$ [60] for photons at 4.4-8.8 GeV ($\sqrt{s} = 3.02$ -4.17 GeV).

From an extensive optical model analysis taking the ratio η_ρ to be -0.2, Alvensleben *et al.* [61] found

$$\sigma_{\text{tot}}(\rho_0 + p) = 26.7 \pm 2 \text{ mb} \quad (50)$$

and $f_\rho^2/4\pi = 4.40 \pm 0.60$ for photons at 4.6-7.2 GeV ($\sqrt{s} = 3.09$ -3.87 GeV). Other measurements give

$$\sigma_{\text{tot}}(\rho_0 + p) = 22.5 \pm 2.7 \text{ mb} \quad (51)$$

with $f_\rho^2/4\pi = 2.52 \pm 0.08$ with $\eta = -0.24$ [62] for photons at 2.75-4.35 GeV ($\sqrt{s} = 2.44$ - 3.01 GeV).

An independent determination of the $\rho - N$ total cross section, using the $\gamma + d \rightarrow \rho + d$ differential cross sections, was carried out by Anderson *et al.* who obtained

$$\sigma_{\text{tot}}(\rho_0 + p) = 27.6 \pm 0.6 \text{ mb} \quad (52)$$

and $f_\rho^2/4\pi = 2.80 \pm 0.12$ at a photon energy of 18 GeV ($\sqrt{s} = 5.98$ GeV) [63].

In our non-relativistic potential model, the ρ and ω have the same spin and spatial wave functions. Consequently, within the two-gluon model of the Pomeron, $\sigma_{\text{tot}}(\rho + p) = \sigma_{\text{tot}}(\omega + p)$. The value of $\sigma_{\text{tot}}(\omega + p)$ extracted from experimental photoproduction data depends again on the coupling constant $f_\omega^2/4\pi$ and η_ω . The extracted values of $\sigma_{\text{tot}}(\omega + p)$ range from 33.5 ± 5.5 mb [64] at 6.8 GeV ($\sqrt{s} = 3.694$ GeV) to 25.4 ± 2.7 mb at 8.3 GeV [65] ($\sqrt{s} = 4.06$ GeV).

Our examination of the experimental $\rho + p$ and $\omega + p$ cross sections at low energies indicates that they appear to range from 23 mb to 38 mb and the uncertainties are large. The cross section depends on energy, and the only data point of $\sigma_{\text{tot}}(\rho + p)$ at $\sqrt{s} = 70$ GeV that can be direct compared with the TGMP model indicates approximate agreement between the theoretical result with experiment. However, much more work needs to be done to confront the predictions of the TGMP and the additive quark model with the results of photoproduction experiments.

For the $\phi + p$ reaction the present results give a theoretical total cross section of 17.1 mb at $\sqrt{s} = 20$ GeV, which agrees with the naive additive quark model of

$$\sigma_{\text{tot}}(\phi + p) = \sigma_{\text{tot}}(K^+ + p) + \sigma_{\text{tot}}(K^- + p) - \sigma_{\text{tot}}(\pi^- + p) \sim 17.0 \text{ mb.} \quad (53)$$

The experimental photoproduction data give a $\sigma_{\text{tot}}(\phi + p)$ which ranges from 9.2 mb to 17.6 mb for photons at 6.4-9.3 GeV ($\sqrt{s} = 3.59 - 4.28$ GeV), depending on the values of $f_\phi^2/4\pi$ and η_ϕ assumed.

The TGMP gives a theoretical total cross section of $\sigma_{\text{tot}}(J/\psi + p) = 7.6$ mb at $\sqrt{s} = 20$ GeV. From the absorption of J/ψ in pA collisions, an effective $J/\psi + p$ dissociation cross section of about 4-6 mb is used to described the dissociation process [3, 4, 5, 6, 7, 8, 9, 10, 11, 12]. For the above analysis of J/ψ production in Pb-Pb collisions at $\sqrt{s} = 17.3$ GeV, the energy at which the J/ψ or its precursor collides with a nucleon is probably about $\sqrt{s} \sim 8$ GeV, corresponding to the collision of a produced J/ψ nearly at rest with an incident nucleon in the nucleon-nucleon center-of-mass system. Thus, a theoretical result of $\sigma_{\text{tot}}(J/\psi + p) = 7.6$ mb in which the predominant component may be the dissociation cross section, is approximately consistent with the experimental dissociation cross section of about 4-6 mb. It remains necessary to determined more quantitatively how the $J/\psi + p$ cross section depends on energy, how much of the total cross section of $J/\psi + p$ can be attributed to dissociation of J/ψ into an open-charm pair, and whether the observed absorption of J/ψ inside a nucleus may involve an admixture of charmonium states with a color-octet component.

The total $J/\psi + p$ cross section can also be extracted from the dipole model of photoproduction [45]. In this model, light cone wave functions for the virtual photon and charmonium are assumed, and a universal dipole cross section is introduced to fit proton structure function at small x and a wide range of Q^2 . The dipole model gives $\sigma_{\text{tot}}(J/\psi + p) = 4.4$ mb at $\sqrt{s} = 20$ GeV, which is lower than the value of 7.6 mb obtained here in the TGMP model.

Experimental data indicate that at high energies total hadron-hadron cross sections increase slowly with energy. This energy dependence is beyond the scope of the present TGMP model. We can include such a dependence phenomenologically, by assuming that the strength parameters of the interaction depend on energy. Specifically, we assume the energy dependence given by Donnachie and Landshoff [1], and parametrize the energy dependence of the interaction strengths as

$$\alpha_s(\sqrt{s}) = \alpha_s(\sqrt{s} = 20 \text{ GeV})f(\sqrt{s}), \quad (54)$$

$$b_0(\sqrt{s}) = b_0(\sqrt{s} = 20 \text{ GeV})f(\sqrt{s}), \quad (55)$$

where

$$[f(\sqrt{s})]^2 = \frac{Xs^{0.0808} + Ys^{-0.4525}}{(Xs^{0.0808} + Ys^{-0.4525}) \Big|_{\sqrt{s}=20 \text{ GeV}}}, \quad (56)$$

$X = 21.70$ mb, $Y = 56.08$ mb, and s is in GeV^2 . The energy dependence of our parameters has been so chosen that theoretical pp cross sections follow the energy dependence of Donnachie and Landshoff's parametrization of the total pp cross section, which represents a very good fit to the experimental pp data.

Using such an energy-dependence, we extend our results to energies near $\sqrt{s} = 20$ GeV and beyond. The lines in Fig. 3 show our results for total cross sections as a function of \sqrt{s} . The symbols of circles, open-triangles, solid-triangles, open-squares, and solid-squares are experimental data for pp , π^-p , π^+p , K^-p , and K^+p [53], respectively. It can be seen that in regions where data are available, our results are consistent with experimental data. Numerical results for total hadron-hadron cross sections are given in Table I.

Recently, from the elastic and proton-dissociative ρ^0 photoproduction data obtained by the ZEUS Collaboration at HERA [66], the non-resonant contributions were analyzed in terms of the fluctuation of a photon into a $\pi^+\pi^-$ pair and their interaction with a nucleon [67]. A model-dependent analysis of the non-resonant contribution by Ryskin *et al.* [67], based on the Drell-Söding approach [68, 69], yields an effective total πp cross section of $\sigma(\pi p) = 31 \pm 2(\text{stat}) \pm 3(\text{syst})$ for a pion-proton center-of-mass energy of about 50 GeV [70]. The data of the ZEUS Collaboration is shown as the solid diamond point in Fig. 3 and is consistent with the present results of Fig. 3.

VI. TOTAL CROSS SECTIONS FOR MIXED-COLOR CHARMONIUM ON A PION OR A PROTON

A charmonium system that is produced in a parton-parton collision may be in a nontrivial color state, out of which different pure color states may be projected [36, 38]. This initial state wave packet may acquire a transverse momentum and will travel through the nuclear medium. It is therefore clearly of interest to study the propagation of a colored $c\bar{c}$ in a color-singlet hadronic medium.

The color wave function of a color-octet meson is

$$|C^{8c}\rangle = \frac{1}{\sqrt{2}} \sum_{\alpha, \beta=1}^3 \lambda_{\alpha\beta}^c |\alpha \bar{\beta}\rangle, \quad (c = 1, 2, \dots, 8). \quad (57)$$

For the scattering of a color-octet meson with a color-singlet meson, we have

$$\sum_{a,b=1}^8 \langle C_I^{8c} | \lambda_i^a \lambda_j^b | C_I^{8d}\rangle \langle C_{II}^1 | \lambda_k^a \lambda_l^b | C_{II}^1\rangle = \begin{cases} \frac{32}{9} \delta^{cd}, & i = j, \\ -\frac{4}{9} \delta^{cd}, & i \neq j, \end{cases} \quad (58)$$

and for the scattering of a color-octet meson with a proton we have

$$\sum_{a,b=1}^8 \langle C_I^{8c} | \lambda_i^a \lambda_j^b | C_I^{8d}\rangle \langle C_{II}^1 | \lambda_k^a \lambda_l^b | C_{II}^1\rangle = \begin{cases} 32/9 \delta^{cd}, & i = j, \quad k = l, \\ -4/9 \delta^{cd}, & i \neq j, \quad k = l, \\ -16/9 \delta^{cd}, & i = j, \quad k \neq l, \\ 2/9 \delta^{cd}, & i \neq j, \quad k \neq l. \end{cases} \quad (59)$$

The color state of a mixed-color meson can be expressed as

$$|C^{mixed-color}\rangle = \gamma_1 |C^1\rangle + \sum_{c=1}^8 \gamma_{8c} |C^{8c}\rangle. \quad (60)$$

For a mixed-color meson scattering on a hadron, we have

$$\begin{aligned} & \sum_{a,b=1}^8 \langle C_I^{mixed-color} | \lambda_i^a \lambda_j^b | C_I^{mixed-color}\rangle \langle C_{II}^1 | \lambda_k^a \lambda_l^b | C_{II}^1\rangle \\ &= \sum_{a,b=1}^8 \left[|\gamma_1|^2 \langle C_I^1 | \lambda_i^a \lambda_j^b | C_I^1\rangle + \sum_{c=1}^8 |\gamma_{8c}|^2 \langle C_I^{8c} | \lambda_i^a \lambda_j^b | C_I^{8c}\rangle \right] \\ & \quad \times \langle C_{II}^1 | \lambda_k^a \lambda_l^b | C_{II}^1\rangle \\ &= |\gamma_1|^2 \left(\sum_{a,b=1}^8 \langle C_I^1 | \lambda_i^a \lambda_j^b | C_I^1\rangle \langle C_{II}^1 | \lambda_k^a \lambda_l^b | C_{II}^1\rangle \right) \\ & \quad + \sum_{c=1}^8 |\gamma_{8c}|^2 \left(\sum_{a,b=1}^8 \langle C_I^{8c} | \lambda_i^a \lambda_j^b | C_I^{8c}\rangle \langle C_{II}^1 | \lambda_k^a \lambda_l^b | C_{II}^1\rangle \right). \end{aligned} \quad (61)$$

From Eqs. (40) — (42) and (61), the total cross section of a mixed-color meson scattering on a hadron can be expressed as [39]

$$\sigma_{tot} = (1 - P_8) \sigma_{tot}^{1+1} + P_8 \sigma_{tot}^{8+1}, \quad (62)$$

where $P_8 = \sum_{c=1}^8 |\gamma_{8c}|^2$ gives the total amount of color-octet mixing.

In Fig. 4(a) and 4(b) we show the total scattering cross sections of a mixed-color charmonium on a pion or on a proton, as a function of the size of the $c\bar{c}$ pair and the amount of color mixing at $\sqrt{s} = 20$ GeV. The wave function of the charmonium state is taken to be a single Gaussian wave function characterized by a root-mean square radius. The cross sections are insensitive to the spin state of the $c\bar{c}$ system. The results in Fig. 4 are the total cross sections for the collision of a spin-triplet $S = 1$ $c\bar{c}$. It can be seen that the total cross section of a color-octet charmonium ($P_8 = 1.0$) scattering on a hadron remains finite even as the size of the charmonium approaches zero, and they change only weakly with the charmonium size. This is quite different from the case of a color-singlet charmonium ($P_8 = 0.0$)

scattering from a color-singlet hadron. For the case of the scattering of two color-singlet mesons, if we turn off the spin-spin interaction, the integrand in Eq. (2) is proportional to

$$[V_T(\mathbf{r}_{1T} - \mathbf{r}_{3T}) + V_T(\mathbf{r}_{2T} - \mathbf{r}_{4T}) - V_T(\mathbf{r}_{1T} - \mathbf{r}_{4T}) - V_T(\mathbf{r}_{2T} - \mathbf{r}_{3T})]^2, \quad (63)$$

and for the case of the scattering of a color-octet meson with a color-singlet meson, the integrand is instead proportional to

$$\begin{aligned} & [V_T(\mathbf{r}_{1T} - \mathbf{r}_{3T}) + V_T(\mathbf{r}_{2T} - \mathbf{r}_{4T}) - V_T(\mathbf{r}_{1T} - \mathbf{r}_{4T}) - V_T(\mathbf{r}_{2T} - \mathbf{r}_{3T})]^2 \\ & + \frac{9}{4} [V_T(\mathbf{r}_{1T} - \mathbf{r}_{3T}) - V_T(\mathbf{r}_{1T} - \mathbf{r}_{4T})][V_T(\mathbf{r}_{2T} - \mathbf{r}_{3T}) - V_T(\mathbf{r}_{2T} - \mathbf{r}_{4T})]. \end{aligned} \quad (64)$$

We can see that expression (64) does not approach zero when the size of the color-octet meson approaches zero ($\mathbf{r}_{1T} \rightarrow \mathbf{r}_{2T}$), unlike expression (63). There are cancellations in the case of color-singlet hadron-hadron scattering, which are not present in the scattering of a color-octet charmonium state on color-singlet hadrons, as first pointed out by Dolejši and Hüfner [32].

The color-octet cross sections for $P_8 = 1.0$ are approximately the same as those of Dolejši and Hüfner [32], even though the potentials used are quite different. For the collision of the color-singlet charmonium ($P_8 = 0.0$) on π and p , the results at $\sqrt{\langle r_{c\bar{c}}^2 \rangle} = 0.2$ fm in Fig. 4 are close to the results for $J/\psi + \pi$ and $J/\psi + p$ in Fig. 2 as the rms radius of J/ψ in our calculation is 0.202 fm.

VII. SUMMARY AND CONCLUSIONS

We have calculated total hadron-hadron cross sections for the collisions of π , K , ρ , ϕ , D , J/ψ , ψ' , Υ , Υ' , and the proton using the Low-Nussinov model of two-gluon exchange, as developed by Gunion, Soper, Landshoff, Nachtmann, Dolejši, Hüfner, and Wong. A set of meson wave functions obtained from a non-relativistic quark potential model is used in our calculations. A phenomenological potential including screened color-Coulomb, screened confining, and spin-spin interactions is employed to describe the gluon exchange between the constituents of the interacting hadrons. The screening mass and the strong coupling constant of the potential are obtained by fitting the total cross sections of $p+p$, $\pi+p$, and $K+p$ collisions at $\sqrt{s} = 20$ GeV. We extend our results to higher energies using the phenomenological energy dependence obtained by Donnachie and Landshoff [1].

We find that the total hadron-hadron cross sections correlate with the size of the scattering hadron system. There are, however, important variations arising from the spin-spin interaction. This leads to $\sigma_{\text{tot}}(\pi + p) > \sigma_{\text{tot}}(K + p)$, a larger ρ rms radius, and consequently a $\sigma_{\text{tot}}(\rho + p)$ that is slightly greater than $\sigma_{\text{tot}}(\pi + p)$. The experimental total $\pi + p$ cross section at 50 GeV obtained by the ZEUS Collaboration agrees with the theoretical result of the TGMP and the experimental ZEUS data point of the total $\rho + p$ cross section at $\sqrt{s} = 70$ GeV is close to the theoretical prediction.

While the TGMP and the additive quark model give about the same cross sections in some cases, there are significant deviations because the effective spatial range of the quark-quark interaction in the present analysis, $1/\mu$, is not small compared to hadron radii. The total $\pi+\pi$, and $\pi+\rho$ cross sections obtained here differ significantly from those of the additive quark model. Much more work remains to be done to confront the predictions of the TGMP and the additive quark model with experiments. It will be of great interest to obtain quantitative experimental measurements of these cross sections, using for example the production of pions in photon-photon collisions in which each photon fluctuates into a pair of pions, as in the Drell [68] and Söding [69] approach in photon reaction processes.

As was previously noted by Dolejši and Hüfner [32], we find that the theoretical total cross section for a color-octet meson is quite large. The large cross section arises from the fact that in the interaction of a color-octet meson, the color interactions of both constituents in the meson interfere constructively, while in a color-singlet meson, the interactions interfere destructively. Therefore, a color-octet meson traveling through a color-singlet nuclear medium is expected to suffer frequent collisions and will lose a substantial amount of energy. These results for the color-octet cross sections may be used to place a constraint on the color-octet production amplitude of a heavy-quark pair produced in a nucleon-nucleon collision by studying its propagation in the nuclear medium.

It will be of interest in future work to study the elastic differential cross section based on the TGMP, which can be compared directly with experiment. It would be useful to develop experimental and theoretical techniques to infer cross sections of unstable mesons on various targets, which would be valuable to discriminate between various theoretical models.

Acknowledgments

The authors would like to thank Drs. T. Barnes, H. Crater, and C. W. Wong for helpful discussions. WNZ would also like to thank Dr. Glenn Young for his kind hospitality at Oak Ridge National Laboratory. This research was supported in part by the Division of Nuclear Physics, U.S. Department of Energy, under Contract No. DE-AC05-00OR22725, managed by UT-Battelle, LLC, and by the National Natural Science Foundation of China under Contract No. 10275015.

-
- [1] A. Donnachie and P.V. Landshoff, Phys. Lett. **B296**, 227 (1992).
 - [2] T. Matsui and H. Satz, Phys. Lett. **B178**, 416 (1986).
 - [3] C. Gerschel and J. Hüfner, Phys. Lett. **B217**, 386 (1989); C. Gerschel and J. Hüfner, Nucl. Phys. **A544**, 513c (1992).
 - [4] C. Y. Wong, Nucl. Phys. **A610**, 434c (1996); Nucl. Phys. **A630**, 487 (1998).
 - [5] C. Y. Wong, hep-ph/9809497, in Proceedings of Workshop on Charmonium Production in Relativistic Nuclear Collisions, (INT, Seattle, May 18-22, 1998).
 - [6] D. Kharzeev, Nucl. Phys. **A610**, 418c (1996); Nucl. Phys. **A638**, 279c (1998).
 - [7] J.-P. Blaizot and J.-Y. Ollitrault, Nucl. Phys. **A610**, 452c (1996).
 - [8] A. Capella, A. Kaidalov, A. K. Akil, and C. Gerschel, Phys. Lett. **B393**, 431 (1997).
 - [9] W. Cassing and C. M. Ko, Phys. Lett. **B396**, 39 (1997); W. Cassing and E. L. Bratkovskaya, Nucl. Phys. **A623**, 570 (1997).
 - [10] R. Vogt, Phys. Lett. **B430** 15 (1998).
 - [11] M. Nardi and H. Satz, Phys. Lett. **B442** 14 (1998).
 - [12] Bin Zhang, C.M. Ko, Bao-An Li, Ziwei Lin, and Ben-Hao Sa, Phys. Rev. **C62**, 054905 (2000).
 - [13] D.B. Blaschke, G. R. G. Burau, M. I. Ivanov, Yu. L. Kalinovsky, and P. C. Tandy, Phys. Lett. **B506**, 297 (2001).
 - [14] K. Martins, D. Blaschke, and E. Quack, Phys. Rev. **C51**, 2723 (1995).
 - [15] C. Y. Wong, E. S. Swanson, and T. Barnes, Phys. Rev. **C62**, 045201, 2000.
 - [16] C. Y. Wong, E. S. Swanson, and T. Barnes, in Proceedings of the Hirscheegg 2000 Workshop on Hadrons in Dense Matter (Hirscheegg, Austria, 16-22 January 2000); nucl-th/000203.
 - [17] T. Barnes, E.S. Swanson, and C.Y. Wong, Proceedings of International Workshop on Heavy Quark Physics 5 (Dubna, 6-8 April 2000), nucl-th/0006012.
 - [18] C.Y. Wong, E.S. Swanson, and T. Barnes, Phys. Rev. **C65**, 014903 (2001).
 - [19] T. Barnes, E.S. Swanson, C.-Y. Wong, and X.-M. Xu, [nucl-th/0302052].
 - [20] X.M. Xu, C.Y. Wong, and T. Barnes, Phys. Rev. **C67**, 014907 (2003).
 - [21] T. Barnes and E. S. Swanson, Phys. Rev. **D46**, 131 (1992); E. S. Swanson, Ann. Phys. (NY) **220**, 73 (1992).
 - [22] D. Kharzeev and H. Satz, Phys. Lett. **B334**, 155 (1994).
 - [23] S. G. Matinyan and B. Müller, Phys. Rev. **C58**, 2994 (1998).
 - [24] K. L. Haglin, Phys. Rev. **C61**, 031912 (2000); K. L. Haglin and C. Gale, Phys. Rev. **C63** 065201 (2001) [nucl-th/0002029].
 - [25] Z. W. Lin and C. M. Ko, Phys. Rev. **C62**, 034903 (2000).
 - [26] C.Y. Wong, T. Barnes, E.S. Swanson, and H.W. Crater, talk presented at Quark Matter Conference 2002, July 18-24, 2002, Nantes, France, to appear in the Proceedings, nucl-th/0209017.
 - [27] C.Y. Wong, E.S. Swanson, and T. Barnes, invited talk presented at Hirscheegg 2000 Workshop, Austria, Hadrons in Dense Matter, 16-22 January 2000, Hirscheegg, Austria, nucl-th/0002034.
 - [28] F. E. Low, Phys. Rev. **D12**, 163 (1975).
 - [29] S. Nussinov, Phys. Rev. Lett. **34**, 1286 (1975).
 - [30] J. F. Gunion and D. E. Soper, Phys. Rev. **D15**, 2617 (1977).
 - [31] P. V. Landshoff and O. Nachtmann, Zeit. Physik, **C35**, 405 (1987).
 - [32] J. Dolejší and J. Hüfner, Z. Phys. **C54**, 489 (1992).
 - [33] J. Hüfner and B. Kopeliovich, Phys. Rev. Lett. **76**, 192 (1996).
 - [34] C. W. Wong, Phys. Rev. **D54**, R4199 (1996).
 - [35] C.Y. Wong, Phys. Rev. **C65**, 034902 (2002).
 - [36] C.Y. Wong, Phys. Rev. **D60**, 114025 (1999).
 - [37] K. Karsch, M.T. Mehr, and H. Satz, Z. Phys. **C37**, 617 (1988).
 - [38] G. T. Bodwin, E. Braaten, and G. P. Lepage, Phys. Rev. D **51**, 1125 (1995).
 - [39] C. Y. Wong, Chin. J. Phys. **35**, 857 (1997), [hep-ph/9712320].
 - [40] C. Y. Wong and C. W. Wong, Phys. Rev. **D57** 1838 (1998).
 - [41] C. Y. Wong, Phys. Rev. **D60**, 114025 (1999).
 - [42] J. Hüfner, B. Z. Kopeliovich, and A. Polleri, Eur. Phys. J. **A11**, 457 (2001).
 - [43] J. Hüfner, B. Z. Kopeliovich, and A. Polleri, talk at the XXXVth Rencontres de Moriond on QCD and Hadronic Interactions, 18 – 25 March 2000, Les Arcs, France, [hep-ph/0012010].
 - [44] E. M. Levin and L. L. Frankfurt, JETP Lett. **2**, 65 (1965); H. J. Lipkin and Scheck, Phys. Rev. Lett. **16**, 71 (1966); J. J.

- J. Kokkedee and L. Van Hove, *Nuovo Cimento* **42A**, 711 (1966).
- [45] J. Hüfner, Yu. P. Ivanov, B. Z. Kopeliovich, and A. V. Tarasov, *Phys. Rev.* **D**, 094022 (2000).
- [46] T.T. Chou and C.N. Yang, *Phys. Rev.* **170**, 1591 (1968).
- [47] T.T. Chou, *Phys. Rev.* **D19**, 3327 (1979).
- [48] E. B. Dally, *Phys. Rev. Lett.* **39**, 1176 (1977).
- [49] E. B. Dally *et al.*, *Phys. Rev. Lett.* **45**, 232 (1980).
- [50] R. C. Walker *et al.*, *Phys. Rev.* **D49**, 5671 (1994).
- [51] L. A. Copley, G. Karl, and E. Obryk, *Nucl. Phys.* **B13**, 303 (1969).
- [52] R. Koniuk and Isgur, *Phys. Rev* **D21**, 1868 (1980)
- [53] K. Hagiwara *et al.*, *Phys. Rev.* D66, 010001 (2002), available on the PDG WWW pages (URL: <http://pdg.lbl.gov/>).
- [54] W.H. Press *et al.*, *Numerical Recipes in Fortran* (Cambridge University Press, 1992).
- [55] T. H. Bauer, R. D. Spital, D. R. Yennie, and F. M. Pipkin, *Rev. Mod. Phys.* **50** 261 (1978).
- [56] A. Pautz and G. Shaw, *Phys. Rev.* **C57**, 2648 (1998).
- [57] N. Bianchi *et al.*, *Phys. Rev.* **C60**, 064617 (1999).
- [58] ZEUS Collaboration, M Derrick *et al.*, *Z. Phys.* **C69**, 39 (1995).
- [59] G. McClellan *et al.*, *Phys. Rev. Lett.* **22**, 377 (1969).
- [60] G. McClellan *et al.*, *Phys. Rev.* **D4**, 2683 (1971).
- [61] H. Alvensleben *et al.*, *Phys. Rev. Lett.* **23**, 1058 (1969).
- [62] P.M. Coddington *et al.*, *Nucl. Phys.* **B95**, 249 (1975).
- [63] R. L. Anderson *et al.*, *Phys. Rev.* **D4**, 3245 (1971).
- [64] H.-J. Behrend *et al.*, *Phy. Rev. Lett.* **24**, 1246 (1970).
- [65] J. Abramson *et al.*, *Phy. Rev. Lett.* **36**, 1428 (1976).
- [66] J. Breitweg *et al.*, the ZEUS Collaboartion, *Eur. J. Phys.* **2**, 247 (1998).
- [67] M. G. Ryskin and Yu. M. Shabelski, *Yad. Fiz.* **61**, 89 (1998), hep-ph/9701407.
- [68] S. Drell, *Phys. Rev. Lett.* **5**, 278 (1960).
- [69] P. Söding, *Phys. Lett.* **19**, 702 (1966).
- [70] The authors are indebted to Dr. M. Arneodo for bringing the ZEUS data for $\pi+p$ at about 50 GeV [66] to their attention.

TABLE I: Numerical results for total hadron-hadron cross sections.

	$\sqrt{s} = 20$ GeV	$\sqrt{s} = 80$ GeV	$\sqrt{s} = 140$ GeV	$\sqrt{s} = 200$ GeV
	σ_{tot} (mb)	σ_{tot} (mb)	σ_{tot} (mb)	σ_{tot} (mb)
p+p	39.118	45.324	49.089	51.785
π +p	24.522	28.412	30.772	32.463
K+p	19.601	22.711	24.597	25.948
J/ψ +p	7.597	8.802	9.533	10.057
$J/\psi + \pi$	3.167	3.669	3.974	4.193
J/ψ +K	3.094	3.585	3.883	4.096
$J/\psi + \rho$	4.703	5.449	5.902	6.226
$\pi + \pi$	27.393	31.739	34.375	36.264
π +K	18.791	21.772	23.581	24.876
K+K	13.402	15.528	16.818	17.742
ρ +p	26.955	31.231	33.825	35.684
$\rho + \pi$	20.801	24.101	26.103	27.537
ρ +K	15.622	18.100	19.604	20.681
$\rho + \rho$	20.397	23.633	25.596	27.002
ϕ +p	17.104	19.818	21.464	22.643
$\phi + \pi$	9.716	11.257	12.192	12.862
$\phi + K$	8.139	9.430	10.214	10.775
$\phi + \rho$	11.610	13.452	14.569	15.370
ψ' +p	15.180	17.588	19.049	20.096
$\psi' + \pi$	5.529	6.406	6.938	7.319
$\psi' + K$	5.577	6.462	6.999	7.383
Υ +p	3.546	4.109	4.450	4.694
$\Upsilon + \pi$	1.423	1.649	1.786	1.884
$\Upsilon + K$	1.460	1.692	1.832	1.933
Υ' +p	10.903	12.633	13.682	14.434
$\Upsilon' + \pi$	3.895	4.513	4.888	5.156
$\Upsilon' + K$	4.050	4.693	5.082	5.361
D +p	18.221	21.112	22.865	24.121
$D + \pi$	13.852	16.050	17.383	18.338
$D + K$	10.540	12.212	13.226	13.953
$D + \rho$	13.435	15.566	16.859	17.786

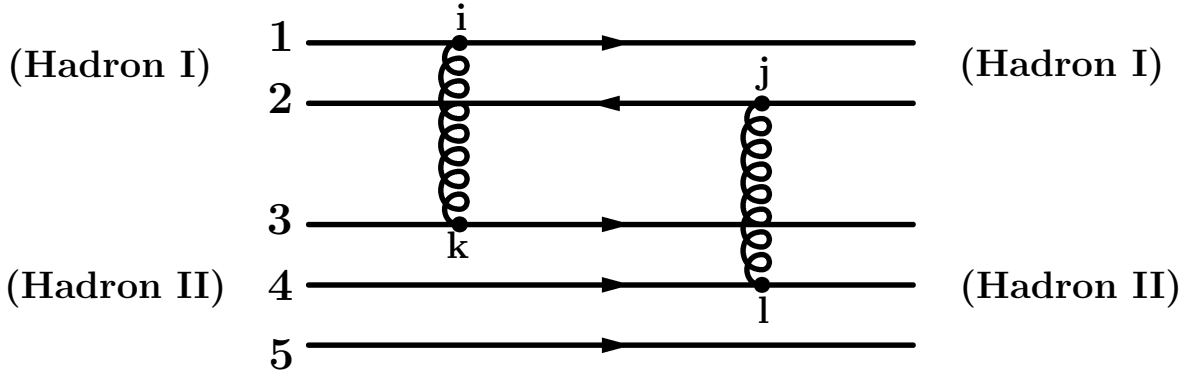


FIG. 1: A two-gluon exchange diagram contribution to the meson-baryon elastic scattering amplitude.

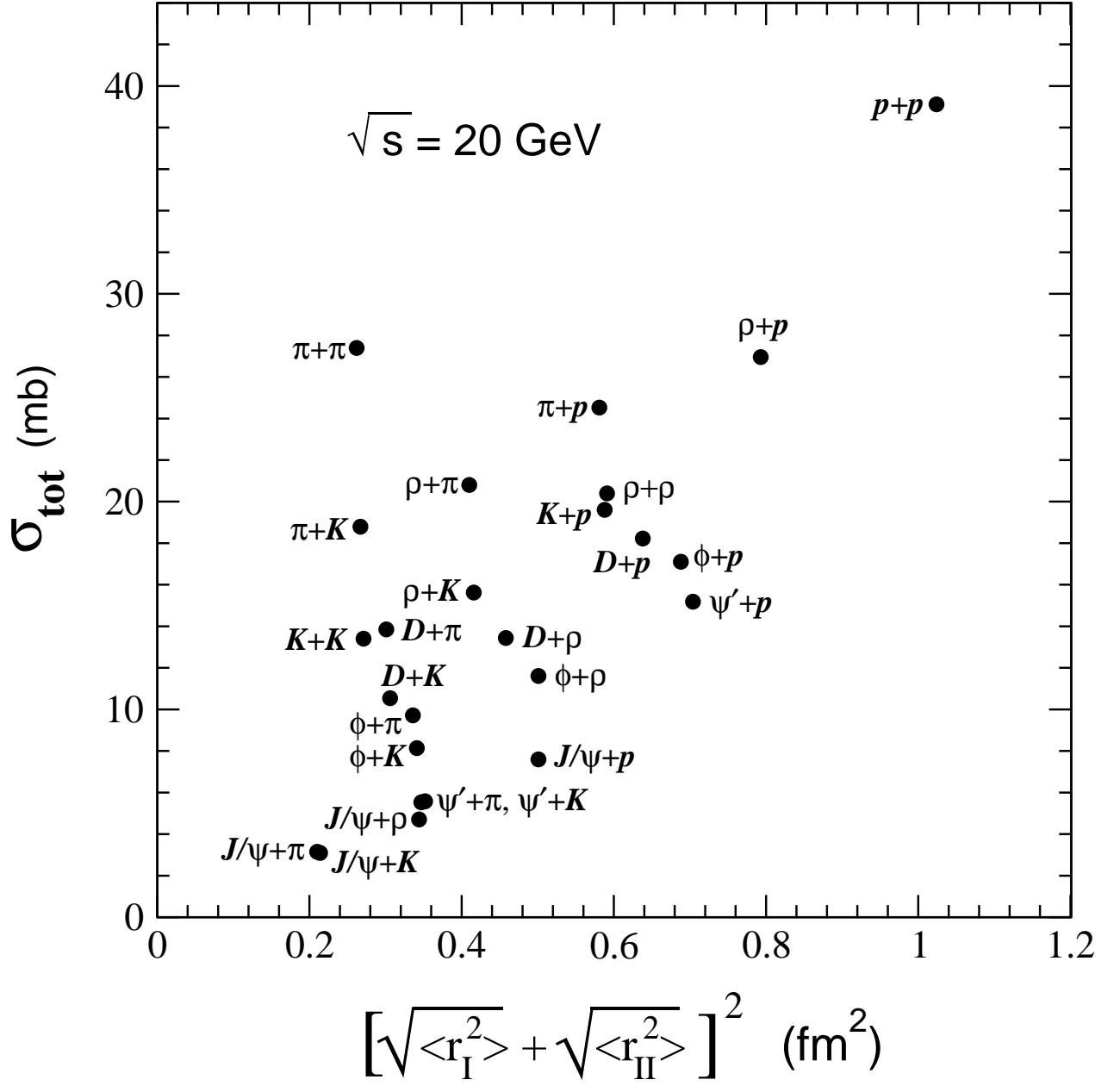


FIG. 2: Total hadron-hadron cross sections as a function of the square of the sum of the rms radii of the colliding hadrons.

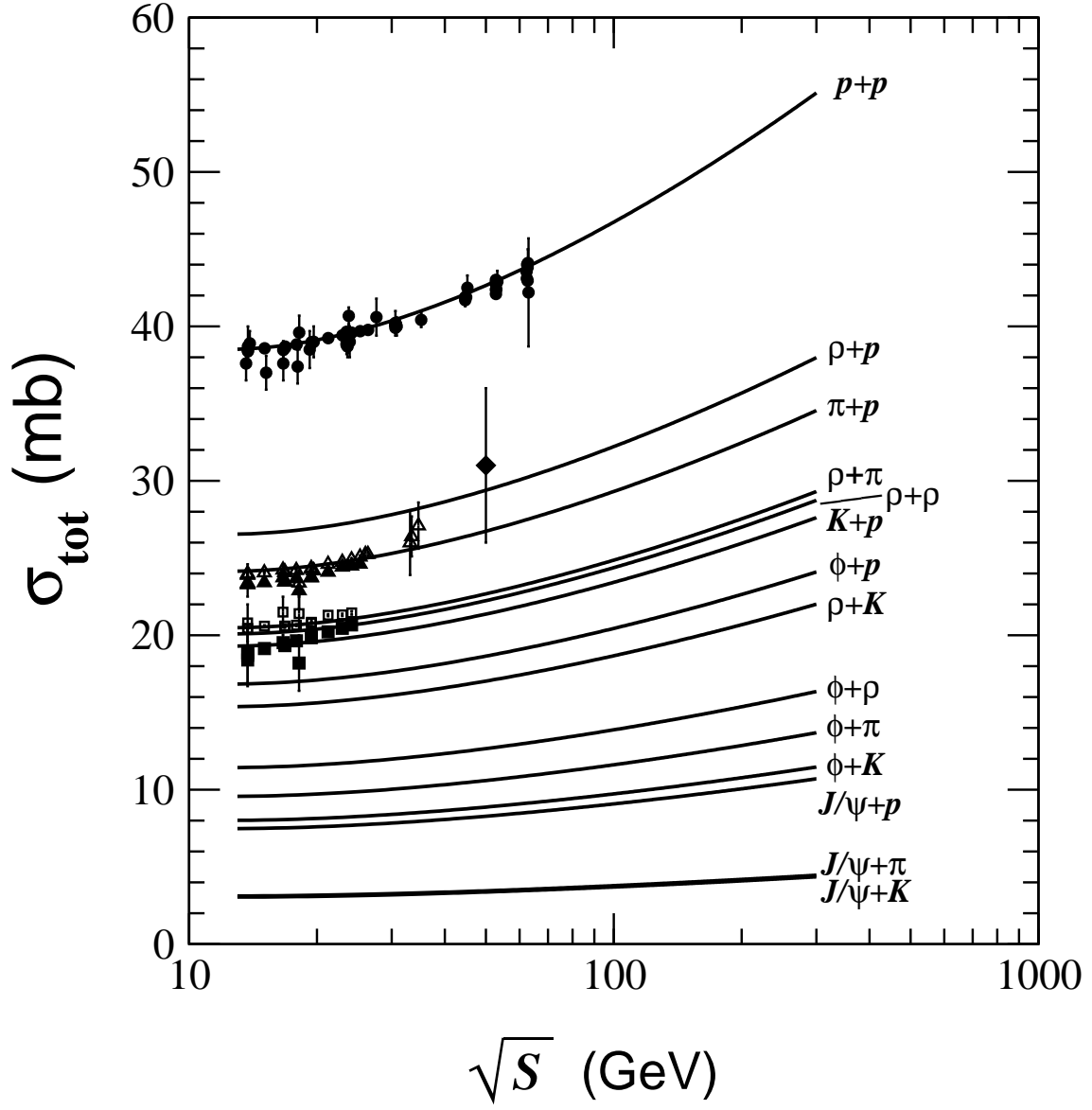


FIG. 3: Total hadron-hadron cross sections as a function of energy. The symbols of circles, open-triangles, solid-triangles, open-squares, and solid-squares represent experimental data for pp , π^-p , π^+p , K^-p , and K^+p [53]. The solid diamond point is from the $\pi+p$ data of the ZEUS Collaboration [66].

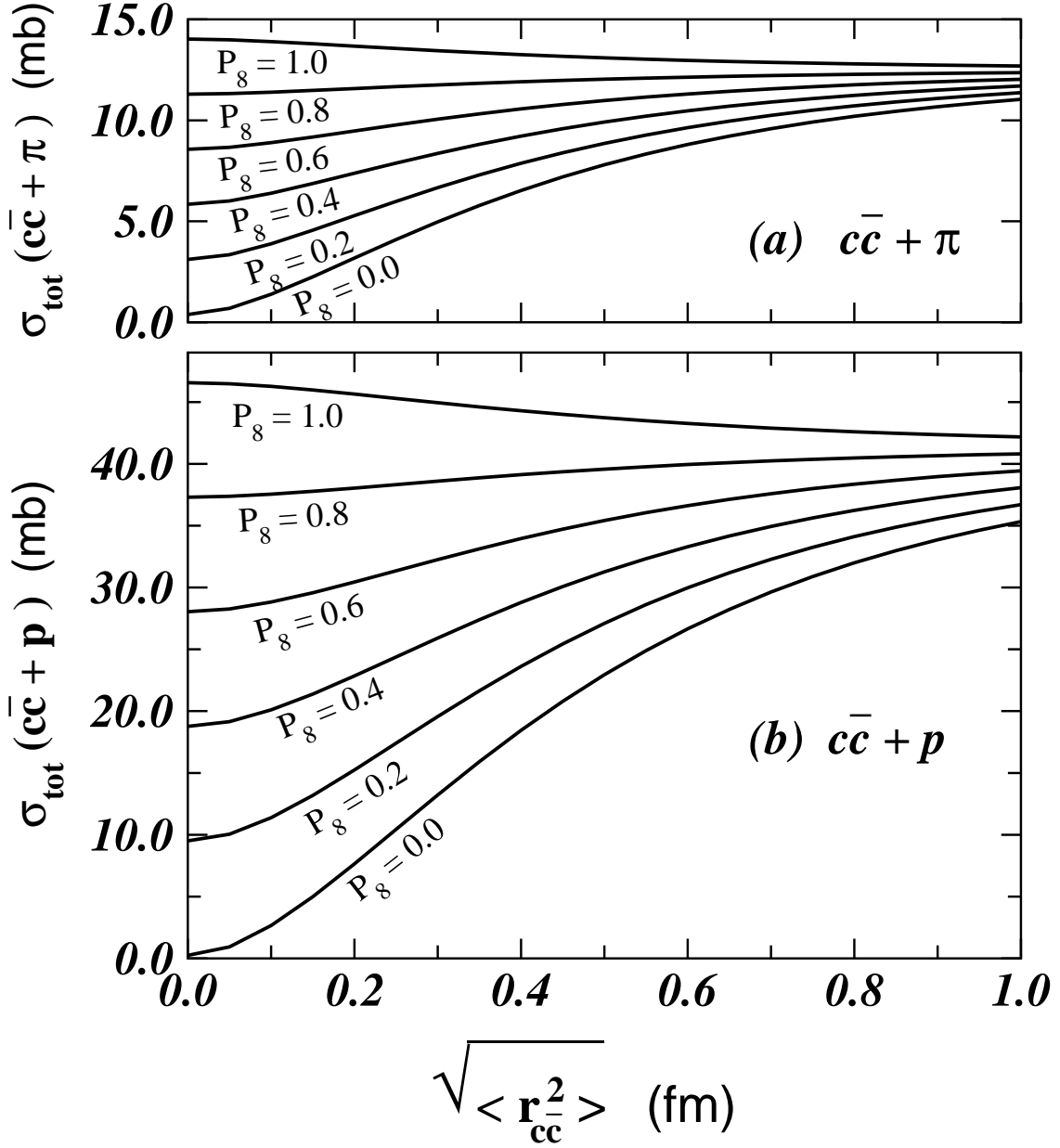


FIG. 4: (a) The total cross sections for mixed-color charmonium scattering on a pion as a function of the charmonium rms radius at $\sqrt{s} = 20$ GeV. P_8 specifies the probability of the charmonium color-octet state. (b) The total cross sections of mixed-color charmonium scattering on a proton as a function of the charmonium rms radius at $\sqrt{s} = 20$ GeV.